Photodissociation of Kr 2 F (4 2 Γ) in the ultraviolet and near-infrared: Wavelength dependence of KrF (B 2 Σ) yield

J. H. Schloss, H. C. Tran, and J. G. Eden

Citation: The Journal of Chemical Physics **106**, 5423 (1997); doi: 10.1063/1.473567
View online: http://dx.doi.org/10.1063/1.473567
View Table of Contents: http://scitation.aip.org/content/aip/journal/jcp/106/13?ver=pdfcov
Published by the AIP Publishing

Photodissociation of $Kr_2F(4\,^2\Gamma)$ in the ultraviolet and near-infrared: Wavelength dependence of KrF ($B\,^2\Sigma$) yield

J. H. Schloss,[a] H. C. Tran,[b] and J. G. Eden
Everitt Laboratory, Department of Electrical and Computer Engineering, University of Illinois, Urbana, Illinois 61801

(Received 27 June 1996; accepted 24 December 1996)

The photoabsorption spectrum of the $4\,^2\Gamma$ excited state of Kr_2F has been measured in the 280–850 nm region by fluorescence suppression spectroscopy. Both the $9\,^2\Gamma \leftarrow 4\,^2\Gamma$ and $6\,^2\Gamma \leftarrow 4\,^2\Gamma$ bands, peaking at 320 and ~710 nm, respectively, have been observed—the latter for the first time. Although the position of the ultraviolet band is consistent with both theory and previous experiments, its spectral width is ~40% of that measured by Greene and McCown [Appl. Phys. Lett. **54**, 1965 (1989)] in absorption experiments in a pulsed discharge. The relative yield of KrF(B) produced in the photodissociation of $Kr_2F(4\,^2\Gamma)$ was found to be independent of wavelength over the 280–360 nm and 590–840 nm spectral intervals and the mechanism responsible for photodissociation appears to be predissociation of the Kr_2F $9\,^2\Gamma$ and $6\,^2\Gamma$ states by potentials correlated with the KrF(D) + Kr and KrF(C) + Kr limits, respectively. © *1997 American Institute of Physics.* [S0021-9606(97)00313-9]

I. INTRODUCTION

The lowest electronic excited state of the rare gas-halide triatomic molecules, denoted $4\,^2\Gamma$, is ionic in character (i.e., $Rg_2^+X^-$, where Rg and X represent rare gas and halogen atoms, respectively) and *ab initio* calculations[1–3] suggest that the effect of the halogen anion on the structural and optical properties of the rare gas dimer cation is negligible. Consequently, the absorption spectra for the $9\,^2\Gamma \leftarrow 4\,^2\Gamma$ and $6\,^2\Gamma \leftarrow 4\,^2\Gamma$ transitions of Kr_2F, for example, are expected to be similar to those for the corresponding transitions of Kr_2^+: $D\,^2\Sigma_g^+ \leftarrow A\,^2\Sigma_u^+$ and $B\,^2\Pi_g \leftarrow A\,^2\Sigma_u^+$, respectively.

Measurements of the photoabsorption cross section for the $4\,^2\Gamma$ state of Xe_2Cl at several wavelengths in the ultraviolet (UV) were described by McCown *et al.*[4] in 1985 and, with the fluorescence suppression approach, McCown[5] and Hakuta and co-workers[6] subsequently determined the $Kr_2F(4\,^2\Gamma)$ absorption cross section at 248 nm. Similar measurements were made by Geohegan and Eden[7,8] for Kr_2F at 35 wavelengths in the 248–572 nm region with a dye laser and were supplemented by continuous scans from 335 to ~600 nm. These results showed that the peak of $Kr_2F(4\,^2\Gamma)$ absorption in the UV lay between 310 and 335 nm. By producing Kr_2F in a transverse discharge, Greene and McCown[9] were able to directly observe $Kr_2F(4\,^2\Gamma)$ in absorption between 225 and 455 nm and confirmed that the $9\,^2\Gamma \leftarrow 4\,^2\Gamma$ band peaks at 315 nm.

In 1988, McCown and co-workers[10] were the first to demonstrate the direct production of the rare gas-fluoride diatomic species when a UV photon is absorbed by the triatomic in the $4\,^2\Gamma$ state. Specifically, these experiments revealed that the photodissociation of $Kr_2F(4\,^2\Gamma)$ in the near-UV (308–351 nm) yields KrF($B\,^2\Sigma$) with a quantum efficiency approaching unity.[11] An analogous observation for $Ar_2F(4\,^2\Gamma)$ was later reported in Ref. 12 but early experiments on Xe_2Cl had searched unsuccessfully for this process.[4]

Experiments in which the $Kr_2F(4\,^2\Gamma)$ absorption spectrum was recorded from 280 to 850 nm are described here. The bands associated with both the $9\,^2\Gamma \leftarrow 4\,^2\Gamma$ and $6\,^2\Gamma \leftarrow 4\,^2\Gamma$ transitions and lying in the UV (280–390 nm) and near-infrared (550–850 nm), respectively, are observed in their entirety. In particular, the $6\,^2\Gamma \leftarrow 4\,^2\Gamma$ absorption band of the molecule which peaks at ~710 nm is observed for the first time and the position and breadth of the band profile are consistent with theoretical predictions. In addition to absorption spectra obtained by fluorescence suppression spectroscopy, the production of KrF excited states by photodissociating $Kr_2F(4\,^2\Gamma)$ was studied by recording the peak KrF($B \rightarrow X$) emission intensity as the excitation wavelength was scanned. A comparison of the absorption (fluorescence suppression) and excitation spectra reveal that the relative yield of KrF(B) in the photodissociation of $Kr_2F(4\,^2\Gamma)$ is independent of wavelength from 280 nm to beyond 800 nm.

II. EXPERIMENT

The experimental apparatus and data acquisition techniques have been discussed in detail previously[8] and will only be reviewed here. A pump–probe approach to selectively examining the optical properties of Kr_2F was adopted in which the initial laser pulse serves to produce the triatomic species. The second, time-delayed (probe) pulse depletes the $Kr_2F(4\,^2\Gamma)$ population by absorption and the observables are the magnitude and wavelength dependence of the $Kr_2F(4\,^2\Gamma \rightarrow 1\,^2\Gamma)$ fluorescence suppression and the concomitant appearance of KrF(B) emission. Briefly, $Kr_2F(4\,^2\Gamma)$ molecules were produced by the beam from an ArF laser (193 nm) which was focused into a quartz cell

[a]Present address: SSI Technologies, Inc., P.O. Box 5011, Janesville, WI 53547.
[b]Present address: Northrop Corp., 600 Hicks Rd., MS-L5300, Rolling Meadows, IL 60008.

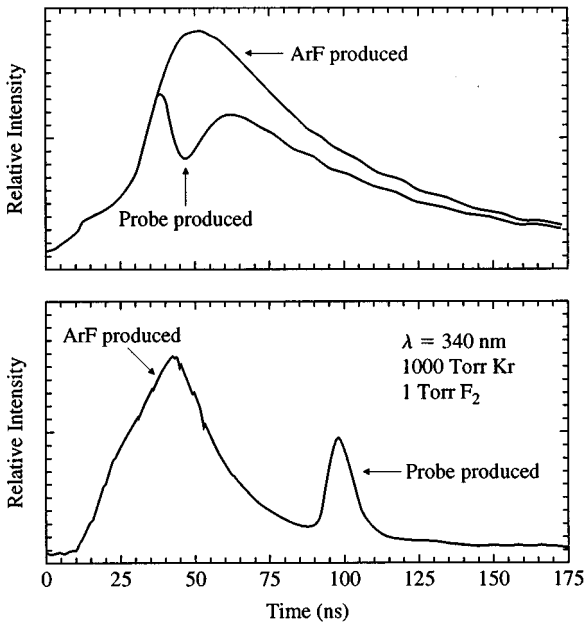

FIG. 1. Typical $Kr_2F(4\,^2\Gamma \rightarrow 1\,^2\Gamma)$ and $KrF(B \rightarrow X)$ emission wave forms: (top) Kr_2F fluorescence wave forms produced by ArF laser irradiation of a 1000 Torr Kr/1 Torr F_2 gas mixture and the suppression of the fluorescence by a dye laser pulse ($\lambda = 340$ nm); (bottom) $KrF(B \rightarrow X)$ emission generated by the ArF laser pulse (early fluorescence peaking at ~40 ns) and the trailing dye laser (probe) pulse. Notice that, for illustrative purposes, Δt is quite different for the two sets of wave forms ($\Delta t \sim 35$ and 90 ns for top and bottom traces, respectively).

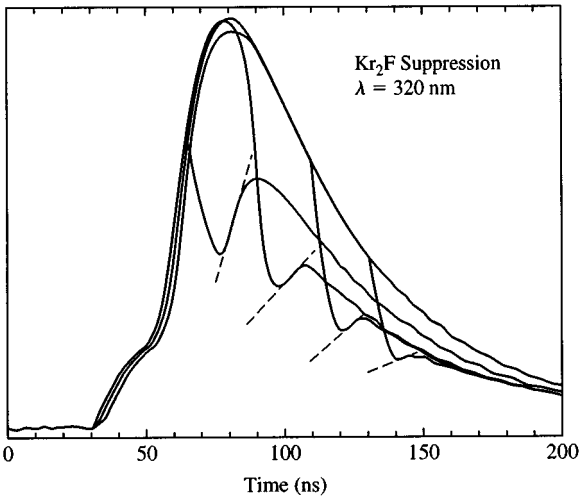

FIG. 2. Five superimposed Kr_2F fluorescence wave forms illustrating the dependence of the suppression profile on Δt for a fixed probe laser intensity and $\lambda = 320$ nm. The dashed lines reflect the slowing of the recovery of the Kr_2F population that results from the rapidly declining $KrF(B,C)$ populations.

containing a room temperature mixture of Kr and F_2. Production of Kr excited states and Kr^+ ions by nonresonant, two photon excitation and 2+1 REMPI, respectively, triggers a series of collisional processes that culminates in the formation of $KrF(B,C)$ and $Kr_2F(4\,^2\Gamma)$. An adjustable time delay (Δt) later, a pulse from an Nd:YAG-pumped dye laser (~10 ns, $\Delta\tilde{\nu} \simeq 0.2$ cm^{-1}, ~1 mm^2 cross-sectional beam area), directed along the axis of the cell and coincident with the focus of the excimer, excites a fraction of the Kr_2F molecules. The absorption of dye laser radiation by $Kr_2F(4\,^2\Gamma)$ is monitored by observing the suppression of $Kr_2F(4\,^2\Gamma \rightarrow 1\,^2\Gamma)$ fluorescence in the violet with a photomultiplier and appropriate optical filters. As noted earlier, the ultimate fate of the Kr_2F species is also of interest; consequently, the relative peak intensity of the $KrF(B \rightarrow X)$ emission produced by the second (dye) laser pulse was also recorded as the laser wavelength was varied. Unless noted otherwise, the gas mixture can be assumed to be 1000 Torr Kr/1 Torr F_2 and Δt is typically set at 60 ns.

III. RESULTS AND DISCUSSION

A. Wave forms, typical data

Fluorescence wave forms representative of those observed throughout these experiments are displayed in Fig. 1. In the upper portion of the figure are shown two oscillograms illustrating $Kr_2F(4\,^2\Gamma \rightarrow 1\,^2\Gamma)$ fluorescence suppression arising from absorption by $Kr_2F(4\,^2\Gamma)$ at 340 nm. In the absence of a probe pulse, the Kr_2F spontaneous emission peaks ~50 ns following the onset of the ArF laser pulse and exhibits a decay time which is consistent with the known spontaneous emission lifetime for the $4\,^2\Gamma$ state and the rate constants for quenching of $Kr_2F(4\,^2\Gamma)$ by Kr and F_2 (Refs. 8 and 13). When the time-delayed probe pulse ($\lambda = 340$ nm) is introduced, strong suppression (~46%) of the Kr_2F fluorescence is observed but note that, following the termination of the probe pulse, the Kr_2F population partially recovers (to >85% of its pre-probe value). In previous experimental studies of Kr_2F absorption by fluorescence suppression, recovery of the Kr_2F population was slight[5] or not detectable,[6–8] an interesting effect that is closely tied to the temporal width of the probe pulse and three body rate constant for Kr_2F formation and which will be discussed in more detail later.

The trace in the lower portion of Fig. 1 shows the $KrF(B \rightarrow X)$ spontaneous emission that is produced by the initial (ArF pump) pulse and the probe radiation ($\lambda = 340$ nm, $\Delta t \simeq 90$ ns). For the remainder of this paper, we will focus on the latter. The temporal history of the KrF fluorescence produced by the probe (dye) laser pulse replicates the dye laser wave form itself; one concludes, therefore, that $Kr_2F(4\,^2\Gamma)$ is converted to $KrF(B)$ on a time scale of $\lesssim 1$–2 ns. A superposition of five Kr_2F fluorescence suppression wave forms, recorded for different values of Δt and a probe laser wavelength of 320 nm, is presented in Fig. 2. Not only do these traces illustrate the reproducibility of the experiment but they also demonstrate that the *rate and degree* of $Kr_2F(4\,^2\Gamma)$ population recovery following the probe pulse (which is reflected by the magnitude of the slope of the wave form during recovery—cf. Fig. 2) falls rapidly as Δt increases. This is precisely what one would expect since the re-formation of $Kr_2F(4\,^2\Gamma)$ depends upon the $KrF(B,C)$ populations, both of which have considerably shorter effective lifetimes than that for $Kr_2F(4\,^2\Gamma)$.

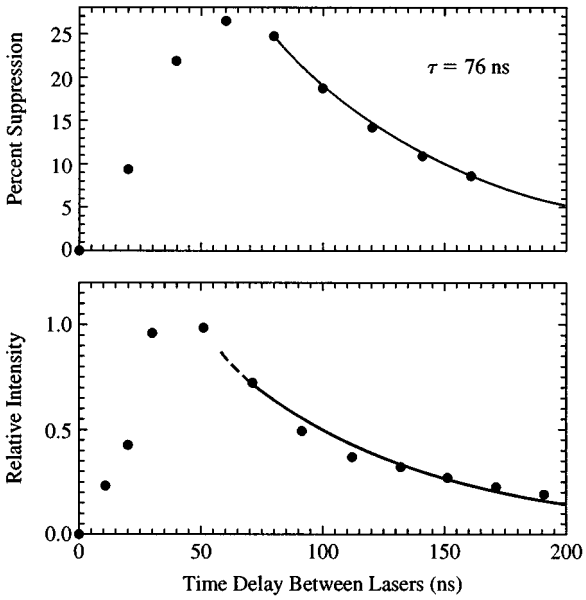

FIG. 3. Comparison of the temporal histories of the: (a) fractional suppression of Kr_2F fluorescence in the violet, and (b) relative peak KrF($B\rightarrow X$) emission, as functions of the time delay, Δt. The decay of both sets of data is well described by a single exponential having a time constant of 76±2 ns for (a) and 74±2 ns for (b). All data were obtained for a probe laser intensity of ~20 MW-cm^{-2}.

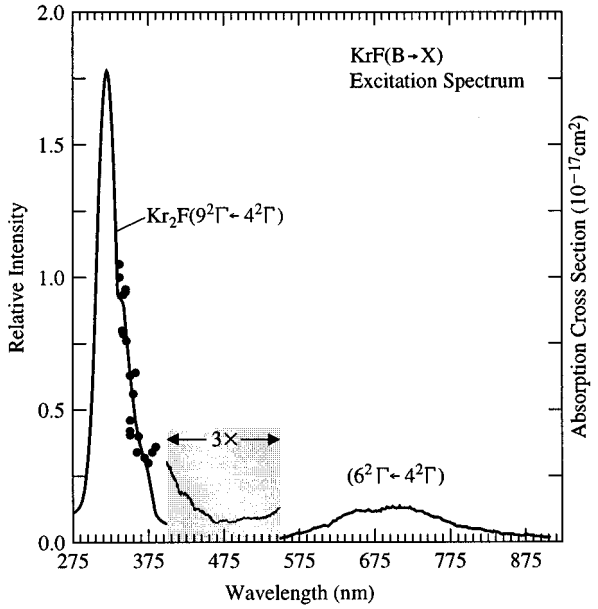

FIG. 4. Excitation spectrum for the production of KrF from $Kr_2F(4\,^2\Gamma)$ in the 280–900 nm region. In acquiring these data, the relative KrF($B\rightarrow X$) emission was monitored and the probe laser intensity was fixed at ~20 MW-cm^{-2}. For the sake of clarity, the 400–550 nm region has been magnified and the data for $\lambda<390$ nm have been smoothed. A few of the Kr_2F ($4\,^2\Gamma$) absorption cross sections in the 337–385 nm interval from Ref. 8 are also shown.

Insight as to the mechanism responsible for the production of KrF(B) is provided by the data of Fig. 3 which compares the magnitude of the Kr_2F violet fluorescence suppression with the peak KrF($B\rightarrow X$) emission intensity as a function of Δt. The fluorescence suppression data were acquired with a probe laser intensity lower than that of Fig. 2 in order to avoid saturating the Kr_2F absorptive transition. Note that the decline in the Kr_2F fluorescence suppression data is well-described by a single exponential having a time constant of 76±2 ns. Similarly, the KrF(B) emission decays exponentially with Δt and, as shown by the solid curve in Fig. 3(b), the time constant that best fits the data is (74±2 ns)$^{-1}$. The fact that the decay constants for both sets of data in Fig. 3 match (to within experimental uncertainty) each other **and** the known effective lifetime of $Kr_2F(4\,^2\Gamma)$ for this gas mixture provides strong evidence that, as suggested by McCown *et al.*,[10,11] the KrF($B\rightarrow X$) fluorescence generated by the probe pulse is, indeed, the result of the photodissociation of $Kr_2F(4\,^2\Gamma)$. Also, results virtually identical to those of Fig. 3 were obtained when the probe laser wavelength was tuned to the expected position[1] of the $Kr_2F(6\,^2\Gamma\leftarrow 4\,^2\Gamma)$ transition in the near-infrared ($\lambda\sim$710 nm)—namely, the suppression of $Kr_2F(4\,^2\Gamma\rightarrow 1\,^2\Gamma)$ spontaneous emission corresponded to the production of KrF(B). Consequently, not only is the $9\,^2\Gamma$ state of Kr_2F unstable with respect to the KrF*+Kr limit (where the asterisk denotes an electronic excited state of the diatomic) but the $6\,^2\Gamma$ state is as well.

B. KrF(B) excitation and $Kr_2F(4\,^2\Gamma)$ absorption spectra

By monitoring the peak KrF ($B\rightarrow X$) emission intensity while scanning the probe laser wavelength, the excitation spectrum for the production of KrF* in the photodissociation of $Kr_2F(4\,^2\Gamma)$ over the 280–900 nm region was obtained and is shown in Fig. 4. Throughout the data acquisition process, the peak intensity of the probe pulse was maintained at 20 MW−cm^{-2} (2 mJ, ~10 ns). Two bands are clearly present in this spectral region, the strongest of which lies in the UV and peaks at ~320 nm. As was discussed earlier, virtually all previous studies of Kr_2F absorption have focused on this band that arises from $9\,^2\Gamma\leftarrow 4\,^2\Gamma$ transitions of the molecule. Aside from the data of Ref. 8 that spanned the 335–600 nm region, the only other $4\,^2\Gamma$ absorption cross sections in the literature were measured at 248 nm (Refs. 5–8), 308 nm (Ref. 8), and 358 nm (Ref. 14). Although the location of the $9\,^2\Gamma\leftarrow 4\,^2\Gamma$ band peak in Fig. 4 is in agreement with the value reported by Greene and McCown[9] (315 nm), our present measurements (as well as the results of Ref. 8) suggest that the bandwidth is only ~33 nm FWHM, or at least a factor two smaller than that given in Ref. 9 (85 nm). The difference may be attributable to the considerably different environments in which the two spectra were recorded. In Ref. 9, Kr_2F was produced in a commercial, transverse discharge device and absorption measurements were made in a 20 ns window during the active discharge or in the early afterglow. It is likely, therefore, that excited vibronic levels of the $Kr_2F(4\,^2\Gamma)$ state populated by electron impact have the effect of significantly broadening the $9\,^2\Gamma\leftarrow 4\,^2\Gamma$ spectrum.

A much weaker band, extending from below 650 nm to beyond 850 nm, is also observed in Fig. 4 and is assigned to the $6\,^2\Gamma\leftarrow 4\,^2\Gamma$ transition of Kr_2F. The existence of this band, which corresponds to the $1(1/2)_g\leftarrow 1(1/2)_u$ transition

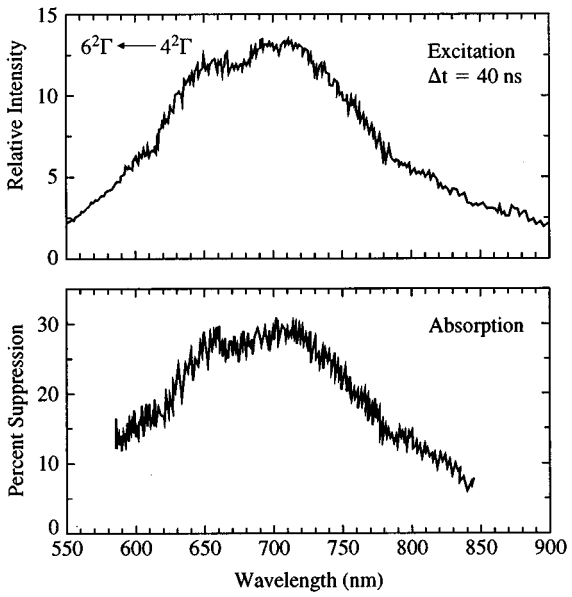

FIG. 5. KrF (B) excitation spectrum (top) and $Kr_2F(4\,^2\Gamma)$ fluorescence suppression (absorption) spectrum in the red and near-IR showing maxima at 655 and 710 nm attributed to the $6\,^2\Gamma \leftarrow 4^2\Gamma$ transition of Kr_2F.

($B\,^2\Pi_g \leftarrow A\,^2\Sigma_u^+$) of the parent Kr_2^+ ion,[1,8] was predicted by Wadt and Hay[1] but, to our knowledge, has not been reported previously. Also, the peak intensity for this band relative to that for the UV band is consistent with the ratio of oscillator strengths calculated in Ref. 1 for the corresponding transitions.

Aside from these two obvious bands, other faint but reproducible structure appears in the 420–490 nm region and in the vicinity of 600 nm. For convenience, the 400–550 nm interval in Fig. 4 has been magnified and, although the signal is too weak to make definitive statements, it is quite possible that these features are associated with the $8\,^2\Gamma \leftarrow 4\,^2\Gamma$ and $7\,^2\Gamma \leftarrow 4\,^2\Gamma$ transitions of Kr_2F that were predicted by Wadt and Hay[1] to peak at 478 and 603 nm, respectively. The latter band appears to be partially blended with the blue tail of the stronger $6\,^2\Gamma \leftarrow 4\,^2\Gamma$ band discussed earlier.

Figure 5 gives a comparison of the KrF(B) excitation spectrum in the 550–900 nm region with the $Kr_2F(4\,^2\Gamma)$ absorption spectrum measured by fluorescence suppression over approximately the same wavelength interval. Although the S/N ratio for the fluorescence suppression data is roughly one half of that for the excitation spectrum, it is nevertheless clear that the two spectra exhibit the same structure. Local maxima at ~655 and 710 nm appear in both spectra and their overall profiles are virtually indistinguishable. Recalling that the excitation spectrum is a measure of the production of KrF* as a function of wavelength, then normalizing the excitation spectrum to the fluorescence suppression (absorption) spectrum provides a measure of the wavelength dependence of the relative yield of KrF* in the photodissociation of $Kr_2F(4\,^2\Gamma)$. Consequently, it is reasonable to conclude that the KrF(B) yield is independent of wavelength in the 590–840 nm region. The same result was obtained for the $9\,^2\Gamma \leftarrow 4\,^2\Gamma$ spectra—the profiles for both the excitation and fluorescence suppression spectra in the 280–360 nm region are essentially identical, indicating that the yield of KrF(B) in this wavelength range is also constant.

The uniform efficiency with which Kr_2F is photodissociated over such a broad spectral range is interesting, particularly in view of the fact that spontaneous emission from Kr_2F excited states higher than $4\,^2\Gamma$ has not been reported in the literature. Diatomics-in-molecules (DIM) calculations carried out by Huestis and Schlotter[2] for the lowest nine electronic excited states of Kr_2F show that all are strongly bound (~2 eV) with respect to the $Kr_2^+ + F^-$ limits. However, only one—$4\,^2\Gamma$—is stable with respect to the KrF(B,C,D)+Kr limits. Specifically, unpublished calculations by Huestis predict that the potentials correlated with $Kr^+F^-(C,D)$+Kr are dissociative. Since: 1) the symmetry species[1] for the KrF($C\,^2\Pi_{3/2}$)+Kr and KrF($D\,^2\Sigma_{1/2}^+$)+Kr limits are $^2B_2$ and $^2A_1$, respectively, and 2) once spin–orbit effects are considered, the $Kr_2F(6\,^2\Gamma)$ state has both $^2A_2$ **and** $^2B_2$ character, then it is likely that the potential associated with KrF(C) +Kr is responsible for predissociation of the $Kr_2F(6\,^2\Gamma)$ state. Similar considerations suggest that $Kr_2F(9\,^2\Gamma)$ (which is almost entirely $^2A_1$ in structure)[1] is predissociated by the repulsive potential arising from KrF(D)+Kr.

It is, therefore, understandable that photoexciting the $9\,^2\Gamma$ state of Kr_2F would rapidly culminate in the production of KrF($B \rightarrow X$) emission. The D and B states of KrF are separated in energy by approximately the spin–orbit splitting of Kr^+ ($^2P_{3/2} - {}^2P_{1/2} \simeq 0.67$ eV). Consequently, the $D\,^2\Sigma_{1/2}^+$ state is ''embedded'' within the B state potential and a number of low $D\,^2\Sigma_{1/2}^+$ vibrational levels are nearly degenerate with $v' < 30$ levels of the $B\,^2\Sigma_{1/2}^+$ state. Furthermore, at the gas pressures typical of these experiments, the B and C states of KrF are closely coupled by collisions—hence, predissociation of the $6\,^2\Gamma$ state of Kr_2F would also quickly produce the KrF(B) species.

C. Modeling of Kr_2F fluorescence recovery: Estimate of KrF yield

In the discussion of Sec. III A, the partial recovery of the $Kr_2F(4\,^2\Gamma)$ fluorescence suppression wave forms following the termination of the probe pulse was noted. One would expect the rate and degree of recovery to depend critically on several kinetic constants; in fact, the experimental wave forms serve as a sensitive and convenient test of the rate constant for the formation of $Kr_2F(4\,^2\Gamma)$ from KrF* by three body collisions and, moreover, allow for a lower limit on the yield of KrF* in the photodissociation of Kr_2F to be determined.

In order to assess the impact of various experimental parameters and rate constants on the fluorescence suppression wave forms, a simple kinetics model of the KrF–Kr_2F system was constructed in which, for convenience, the photodissociation of Kr_2F ($4\,^2\Gamma$) was assumed to produce the KrF (C) species. Photoexcitation of Kr_2F can be described by the following set of three coupled rate equations:

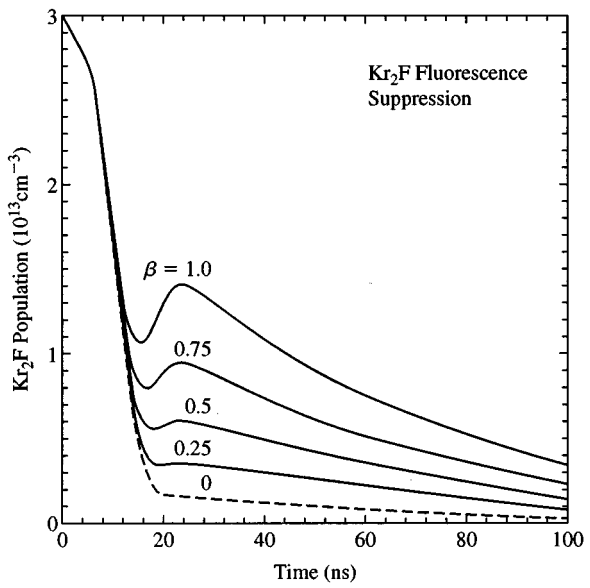

FIG. 6. Simulated $Kr_2F(4\,^2\Gamma)$ fluorescence suppression wave forms illustrating the dependence of the recovery on the KrF(C) quantum yield, β. The actual dye (probe) laser wave form was incorporated into the computations and the peak probe laser intensity was assumed to be 20 MW-cm^{-2}. The initial $Kr_2F(4\,^2\Gamma)$ and KrF(B,C) number densities were set at 3×10^{13} cm^{-3} and zero, respectively, and the probe laser wavelength was 337 nm ($9\,^2\Gamma\leftarrow4\,^2\Gamma$).

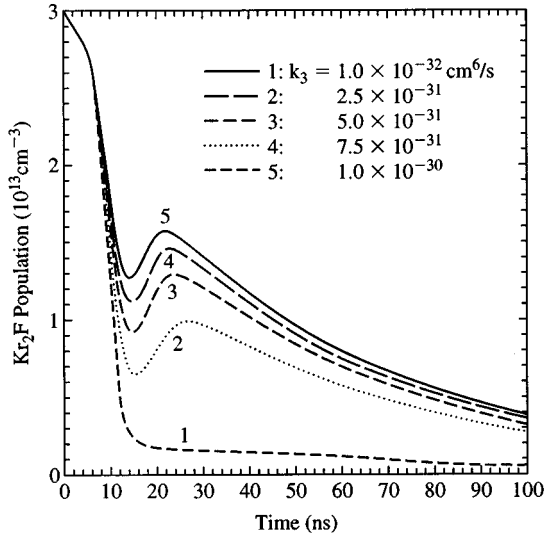

FIG. 7. $Kr_2F(4\,^2\Gamma)$ fluorescence suppression wave forms calculated for five values of the three body Kr_2F formation rate constant k_3, ranging from 10^{-32} cm^6 s^{-1} to 10^{-30} cm^6 s^{-1}.

$$\frac{\partial[\mathrm{KrF}(B)]}{\partial t}=-k_3[\mathrm{Kr}]^2[\mathrm{KrF}(B)]-\frac{[\mathrm{KrF}(B)]}{\tau_b}+k_m\{[\mathrm{KrF}(C)]-[\mathrm{KrF}(B)]\},\tag{1}$$

$$\frac{\partial[\mathrm{KrF}(C)]}{\partial t}=k_m\{[\mathrm{KrF}(B)]-[\mathrm{KrF}(C)]\}+\frac{\sigma I(t)}{\hbar\omega}\beta[\mathrm{Kr_2F}]-\frac{[\mathrm{KrF}(C)]}{\tau_c},\tag{2}$$

$$\frac{\partial[\mathrm{Kr_2F}]}{\partial t}=-k_q[\mathrm{F_2}][\mathrm{Kr_2F}]-\frac{[\mathrm{Kr_2F}]}{\tau_3}+k_3[\mathrm{Kr}]^2[\mathrm{KrF}(B)]-\frac{\sigma I(t)\beta}{\hbar\omega}[\mathrm{Kr_2F}],\tag{3}$$

where brackets denote number densities, $[Kr_2F]$ represents the population of the $4\,^2\Gamma$ state, k_3 is the three body formation rate constant for Kr_2F (6.7×10^{-31} cm^6 s^{-1}), τ_b is the B state spontaneous emission lifetime (6.8 ns), k_m is the rate constant for the mixing of the B and C states by two body collisions with Kr (5×10^{-10} cm^3 s^{-1}), τ_c is the C state radiative lifetime (75 ns), k_q is the rate constant for the quenching of $Kr_2F(4\,^2\Gamma)$ by F_2 (4.3×10^{-10} cm^3 s^{-1}), τ_3 is the $Kr_2F(4\,^2\Gamma)$ spontaneous emission lifetime (178 ns), and β is the quantum yield of KrF(C) in the photodissociation of $Kr_2F(4\,^2\Gamma)$ (Refs. 11, 13, 15, and 16).

A series of five simulated Kr_2F fluorescence suppression wave forms are shown in Fig. 6 for β varied from 0 to 1. In these computations, it was assumed that the probe laser wavelength and peak intensity are 337 nm and 20 MW cm^{-2}, respectively. Also, the initial Kr_2F ($4\,^2\Gamma$) number density is taken to be 3×10^{13} cm^{-3} while the initial KrF(B,C) populations are set to zero. When β=0, re-feeding of the Kr_2F ($4\,^2\Gamma$) state does not occur and, on the basis of a comparison with experimental wave forms, it is clear that β must be $\geqslant$0.75. This result is consistent with the conclusions reached by McCown[11] who measured β for the photodissociation of both Kr_2F and Xe_2Cl in the 193–351 nm spectral interval. For Kr_2F, the branching ratio was determined to 0.9 ± 0.1 between 308 and 351 nm but vanished at 248 and 193 nm. Consequently, the result reported here—that β is constant in the 280–360 nm and 590–840 nm regions—is in agreement with the data of Ref. 11.

The model-generated fluorescence suppression wave forms are also sensitive to the temporal width of the probe laser pulse and to the assumed value for the rate constant k_3. Most of the previous measurements of $Kr_2F(4\,^2\Gamma)$ absorption cross sections by fluorescence suppression have involved an excimer laser or excimer laser-pumped dye laser having pulsewidths in excess of 20 ns. Since this is large compared to the effective KrF(B) lifetime for the gas mixtures of interest here, the simulations confirm prior observations[5–7] that little recovery of the Kr_2F fluorescence following the termination of the probe laser pulse is to be expected. Only as the probe pulsewidth falls below 10 ns [i.e., becoming comparable to the KrF(B) lifetime] does recovery of the wave form become observable. The results of Fig. 7 illustrate the sensitivity of the degree and rate of fluorescence recovery to k_3. Values in the literature for this rate constant differ by more than an order of magnitude but it is clear from the simulated wave forms that accounting for the experimental data requires that k_3 be $\geqslant5\times10^{-31}$ cm^6 s^{-1}. Finally, the influence of re-feeding of the Kr_2F state is clearly illustrated by Fig. 8 in which the variation of the *measured* fluorescence suppres-

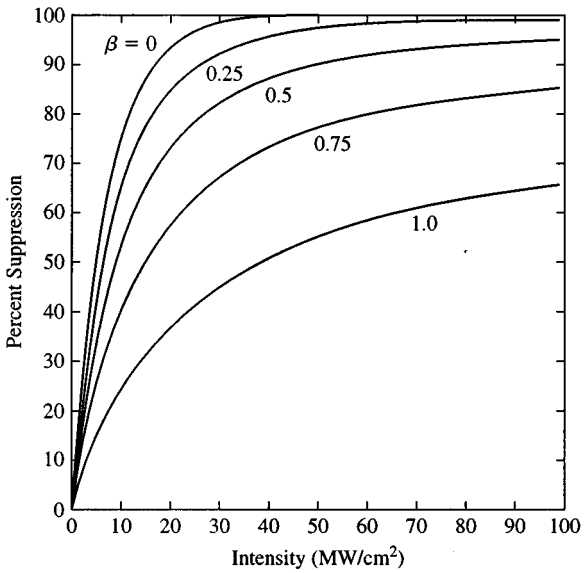

FIG. 8. Calculated dependence of the percentage fluorescence suppression on the probe laser intensity. The results are shown for five values of β. The actual dye laser wave form was incorporated into the simulations.

sion on probe laser intensity is shown for five values of β. Not surprisingly, as the efficiency for replenishing the $Kr_2F(4\,^2\Gamma)$ population is increased ($\beta \rightarrow 1$), the apparent (measured) absorption cross section is smaller than the true value and the effect is most pronounced at low probe laser intensities. However, it should be mentioned that the magnitude of the correction for this effect is reduced dramatically for longer probe laser pulses.

IV. SUMMARY AND CONCLUSIONS

Photodissociation of the $4\,^2\Gamma$ state of Kr_2F has been studied in the 280–850 nm wavelength region by fluorescence suppression and laser excitation spectroscopy. Bands attributed to the $9\,^2\Gamma \leftarrow 4\,^2\Gamma$ ($\lambda_{max} \sim 320$ nm) and $6\,^2\Gamma \leftarrow 4\,^2\Gamma$ ($\lambda_{max} \sim 710$ nm) transitions of the molecule have been observed, the latter for the first time. Weaker features lying in the blue (420–490 nm) and orange (~600 nm) regions of the spectrum were also detected and tentatively assigned to transitions terminating on the $8\,^2\Gamma$ and $7\,^2\Gamma$ states, respectively, of the triatomic.

Photoexcitation of $Kr_2F(4\,^2\Gamma)$ in the UV or near-IR results in dissociation of the molecule and the production of a KrF fragment in the *C* or *D* excited states. Comparing the Kr_2F absorption (fluorescence suppression) and KrF(*B*) excitation spectra demonstrate that the quantum yield for KrF* production is independent of wavelength in the 280–360 nm and 590–840 nm intervals. Modeling of the experimental fluorescence suppression wave forms indicates that the quantum yield for the process: $Kr_2F(4\,^2\Gamma)+\hbar\omega$ (3.4–4.4 eV)$\rightarrow Kr_2F(9\,^2\Gamma) \rightarrow KrF(D)+Kr$ is $\geqslant 0.75$. These results largely confirm the predictions of *ab initio* calculations concerning the positions and relative strengths of Kr_2F absorption bands as well as predissociation of the $6\,^2\Gamma$ and $9\,^2\Gamma$ excited states.

ACKNOWLEDGMENTS

Several valuable discussions with A. W. McCown and D. P. Greene and the expert technical assistance of K. Kuehl, K. Voyles, L. Cliff, D. Prest, and J. Sexton are gratefully acknowledged. This work was supported by the National Science Foundation and the Office of Naval Research.

[1] W. R. Wadt and P. J. Hay, J. Chem. Phys. **68**, 3850 (1978).
[2] D. L. Huestis and N. E. Schlotter, J. Chem. Phys. **69**, 3100 (1978).
[3] W. J. Stevens and M. Krauss, Appl. Phys. Lett. **41**, 301 (1982).
[4] A. W. McCown, M. N. Ediger, D. B. Geohegan, and J. G. Eden, J. Chem. Phys. **82**, 4862 (1985).
[5] A. W. McCown, Appl. Phys. Lett. **50**, 804 (1987).
[6] K. Hakuta, H. Komori, N. Mukai, and H. Takuma, J. Appl. Phys. **61**, 2113 (1987).
[7] D. B. Geohegan and J. G. Eden, Chem. Phys. Lett. **139**, 519 (1987).
[8] D. B. Geohegan and J. G. Eden, J. Chem. Phys. **89**, 3410 (1988).
[9] D. P. Greene and A. W. McCown, Appl. Phys. Lett. **54**, 1965 (1989).
[10] A. W. McCown, D. P. Greene, J. H. Schloss, and J. G. Eden, Paper ThA6, Conference on Lasers and Electro-Optics '88 (CLEO '88), Anaheim, CA (April, 1988).
[11] A. W. McCown, J. Phys. Chem. **94**, 8913 (1990).
[12] K. Hakuta, S. Miki, and H. Takuma, J. Opt. Soc. Am. B**5**, 1261 (1988).
[13] D. L. Huestis, G. Marowsky, and F. K. Tittel, in *Excimer Lasers*, 2nd ed., edited by C. K. Rhodes (Springer, Berlin, 1984), pp. 181–215.
[14] J. G. Eden, R. S. F. Chang, and L. J. Palumbo, IEEE J. Quantum Electron. QE-**15**, 1146 (1979).
[15] J. G. Eden, R. W. Waynant, S. K. Searles, and R. Burnham, Appl. Phys. Lett. **32**, 733 (1978).
[16] P. J. Hay and T. H. Dunning, J. Chem. Phys. **66**, 1306 (1977).